Grenze International Journal of Engineering and Technology, January Issue

Analysing the Changing Trends of Aerosol Optical Depth (AOD) using 6S Radiative Transfer Model for Chennai City

Jeevitha B[1], S. Jayalakshmi[2] and S.S. Shri Darshini[3]
[1-3]Institute of Remote Sensing, College of Engineering Guindy, Anna University, Chennai, India;
Email: balaramanjeevitha@gmail.com, j_lak2001@yahoo.co.in, shridarshiniss@gmail.com

***Abstract*— Increase in urbanization in metropolitan cities like Chennai is leading to decrease in air quality and an increase in the particulate emissions in the air year by year. Monitoring of aerosols is difficult due to the limited number of ground stations, large data gaps, and lower-resolution aerosol products. This study is carried out to overcome the existing spatial resolution limitation of aerosol optical depth retrieval by merging High spatial resolution data Landsat 8 Operational Land Imager with Moderate Resolution Imaging Spectroradiometer surface reflectance data MOD09GA. The 6S radiative transfer model is used for radiative transfer simulation for the existing conditions of Chennai. A lookup table is prepared based on the input parameters given and the Aerosol Optical depth is estimated using an inversion model utilizing surface reflectance from MODIS data. Aerosol Optical Depth maps are retrieved from 2015-2023 to perform trend analysis and the map is compared and validated with ground-based sensor Particulate Matter data acquired from the Central Pollution Control Board to determine the accuracy of retrieval. The validation shows that the Aerosol Optical depth retrieval approach yields a R2 value of 70.35% indicating a higher correlation between the retrieved Aerosol Optical depth value and ground-based PM2.5 data.**

***Index Terms*— Aerosol optical depth, Particulate matter, Landsat 8, Moderate Resolution Imaging Spectroradiometer and Radiative transfer model.**

I. INTRODUCTION

Aerosols are suspended particles in the air that affect the global climate in both direct and indirect ways. They are also seen as a serious threat to human health causing various respiratory diseases and breathing problems. Due to the irregular distribution and non-availability of aerosol measuring ground stations globally, AOD distribution maps at high spatial and temporal are unavailable. The constraints could be addressed by employing satellite remote sensing, which offers an efficient method for examining the spatial patterns and changes of aerosols over extensive periods and large geographical areas. This is achieved by identifying key optical properties of aerosols, such as aerosol optical depth. The targeted study area, Chennai from 2007 to 2018, had a hike of 26.30% in AOD levels (Swagata Payra et al. 2021). Radiative transfer theory is widely used to retrieve AOD from optical remote sensing. One of the widely used methods is the Dense Dark Vegetation method (Tian 2016). The retrieval of AOD is affected by the precise estimation of Land Surface Reflectance, the elimination of cloud cover, and the selection of a suitable aerosol model.

Grenze ID: 01.GIJET.11.1.501
© Grenze Scientific Society, 2025

Accurate estimation of these parameters resulted in a strong correlation with AERONET measurements (Wei et al. 2018). Resolution of the satellite imageries also plays a major role in AOD retrieval using remote sensing (Sun et al. 2015).

II. Study Area

Chennai is the fourth largest metropolitan city in India which is the capital city of Tamil Nadu. Its geographical extent is 12° 51' 3" N to 13° 18' 2" N latitude and 80° 00' 00" E to 80° 14' 15" E longitude (Fig .1). Chennai Metropolitan Area (CMA) covers 8 municipalities, 11 town panchayats and 179 village panchayats in which 10 Panchayat Unions with an area of 1189 Sq.km. The CMA spans three districts in Tamil Nadu, including Chennai, Thiruvallur, and Kancheepuram. CMA is divided into four regions such as North, Central, South and West. The North and Central Chennai are the industrial and commercial sectors of the city respectively. South and West Chennai are known as residential sectors which are now changing into a commercial sector. The city has diversified land use/land cover changes. Over the past few decades, Chennai has faced environmental challenges associated with its significant urbanization, leading to concerns like air pollution. Monitoring air quality has become a crucial undertaking to address potential health risks linked to pollution. Regular assessment of atmospheric conditions in the city is essential for identifying and mitigating the impact of pollutants on public health.

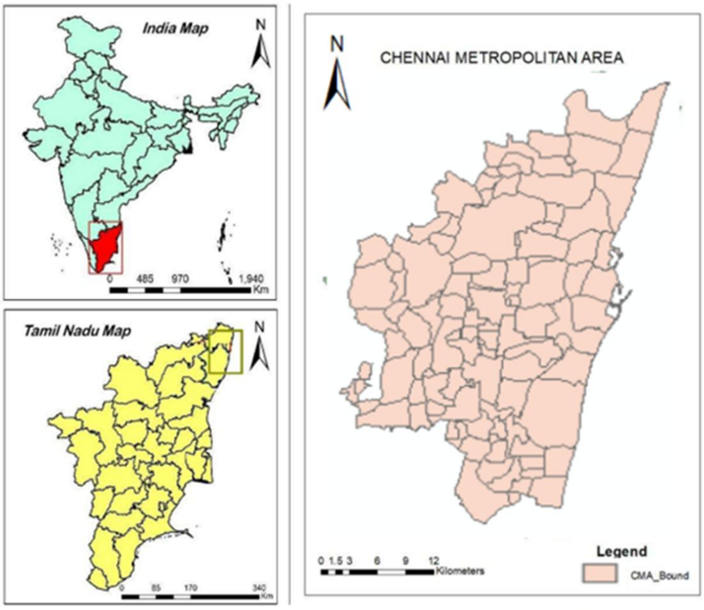

Figure 1. Chennai Study Area

III. Methodology

The accurate estimation of Land Surface Reflectance is one of the influencing factors in the determination of AOD. This study mainly focuses on the retrieval of Surface Reflectance from Moderate Resolution Imaging Spectroradiometer (MODIS) daily product and Top of Atmosphere (TOA) reflectance from LANDSAT 8 for two bands – Blue and Red and implementing this in a Radiative Transfer Model. Integration of Landsat-8 and MODIS databases improved spatial and temporal resolution but introduced inaccuracies due to different geometries (Sun et al. 2015). The detailed methodology of the study is depicted in Figure 2.

A. Estimation of Land Surface Reflectance

The study area Chennai is an urban area with maximum bright pixels and scattered dark pixels such as vegetation and water bodies. The retrieval of AOD in bright pixels has been challenging because in these regions the land surface contribution to radiance received by satellite is larger than the radiance received by vegetation (Sun et al. 2015). It is difficult to estimate surface reflectance with high precision, hence in these regions, blue band is used (Bilal et al. 2013; Li and Yang 2014); Alexei Lyapustin et al. 2011). Even though the Land surface reflectance is more in other bands it remains less than 0.15 in the blue band. This allows AOD retrieval with reasonable precision by determining the Land surface reflectance accurately. Red band surface reflectance has been used for retrieval over dark pixels. The monthly minimum reflectance technique for AOD retrieval over this specific area was applied to the MOD09GA product. To reduce the computation, a one-month land surface reflectance (LSR) database was created for the AOD retrieval data for that month (Wei et al. 2017; Lin et al. 2021). To mitigate the influence of cloud cover and surface contamination, the pixel with the lowest LSR was selected from each of the four images to represent the corresponding pixel in the monthly series. (Omari and Abuelgasim 2019). The cloud-free images were selected for reference LSRs. A synthetic image was generated by combining selected monthly images, where each pixel in the synthetic image corresponds to the minimum surface reflectance observed across all monthly selections. Consequently, monthly constructed images representing LSR of the 8 years from 2015 to 2023 were prepared.

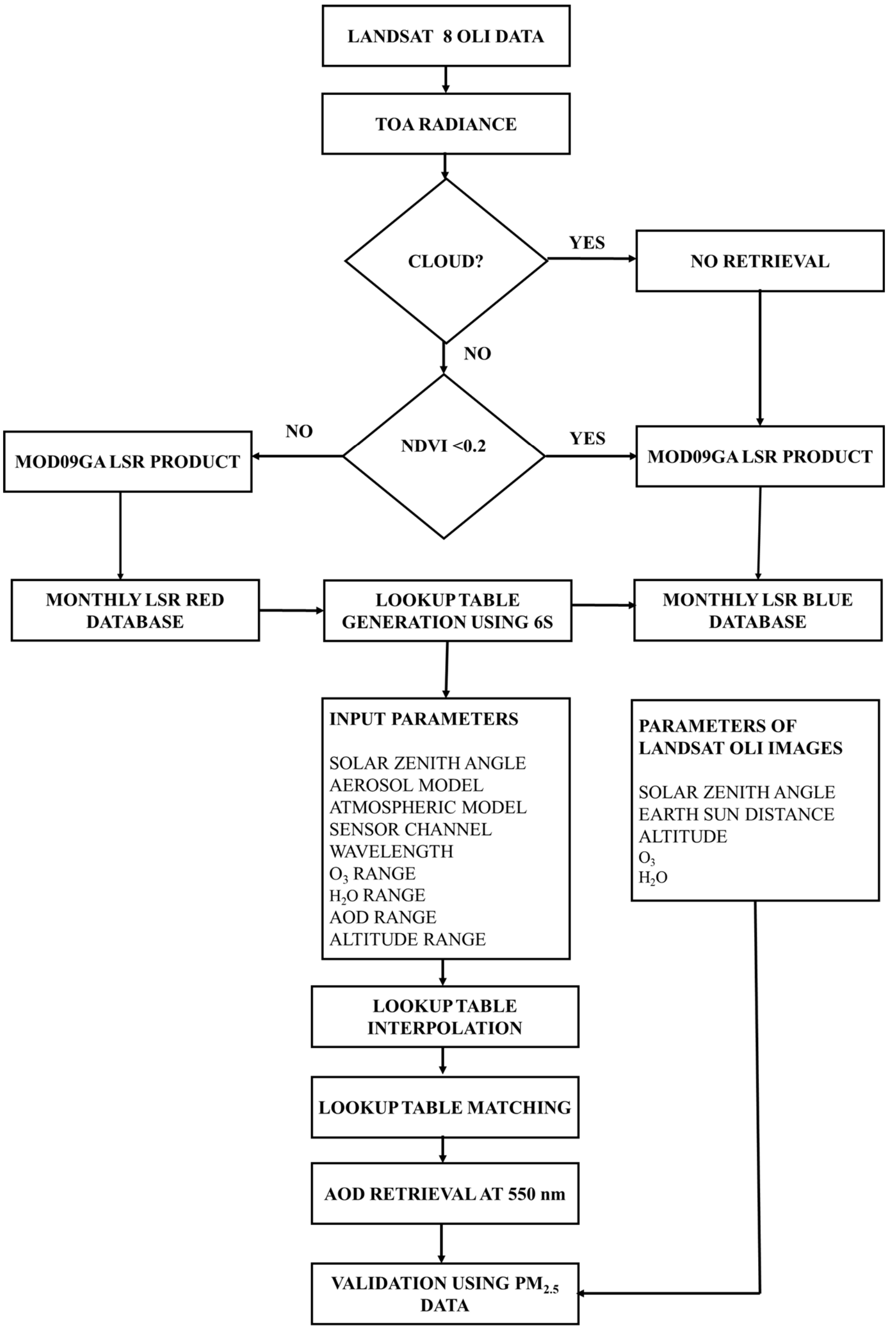

Figure 2. Methodology Flowchart

B. Estimation of Top of Atmosphere Radiance

TOA refers to the radiant energy in the Earth's atmosphere in remote sensing applications. This measurement represents the total radiance reaching a sensor and is expressed in watts per square meter per steradian (W/(m²·sr)). TOA radiance has been calculated for both the red and blue bands of Landsat-8 OLI images (Sun et al. 2015) using Equation (1).

$$\boldsymbol{L_{\lambda} = (M_{L*}Q_{cal}) + A_L} \tag{1}$$

WHERE: $L_{\wedge}$ = TOA SPECTRAL RADIANCE$(Watts/(m^2 * srad * \mu m))$
$M_L = Band - specific\ mulitplicative\ rescaling\ factor$
$RADIANCE\_MULT\_BAND\_x,\ where\ x\ is\ the\ band\ number$
$A_L = Band - specific\ additive\ rescaling\ factor$
$RADIANCE\_ADD\_BAND\_x,\ where\ x\ is\ the\ band\ number$
$Q_{cal} = Quantized\ and\ calibrated\ standard\ product\ pixel\ values\ (DN)$
The Landsat-8 Operational Land Imager (OLI) imagery was resampled to a spatial resolution of 500 meters to align with the resolution of MODIS data. (Chen et al. 2020).

C. Generation of Look-Up Table

The 6S (Second Simulation of Satellite Signal in Solar Spectrum) model code has been used for look-up table generation. It is originally available in the FORTRAN language.
Py6S, which is an interface of the 6S model (Wilson 2013), was used to run the atmospheric Radiative Transfer Model through the Python programming language. Initially, the look-up table was generated using the look-up table (LUT) Build code for the input parameters (Vermote et al. 1997). The radiative transfer model simulates TOA reflectance using the atmospheric scattering of solar radiation and the LSR underneath (Omari and Abuelgasim 2019). For Lambertian surfaces under a plane-parallel atmospheric environment, the radiance detected by a satellite sensor is mathematically formulated as a dependent function of surface reflectance (Tanre et al. 1979), represented by Equation (2).

$$\boldsymbol{L_{(\tau_a, \mu_v \mu_s, \emptyset)} = L_{0(\tau_a, \mu_v, \mu_s, \emptyset)} + \frac{\rho_s}{(1-\rho_s * S(\tau_a))} \mu_s F_0 T(\tau_a, \mu_s) T(\tau_a, \mu_v)} \tag{2}$$

where: L = Radiance at the top of the atmosphere
$\tau_a = Atmospheric\ optical\ depth\ produced\ by\ gas\ molecules\ and\ aerosol$
$L_0 = Path\ radiance\ produced\ by\ scattering\ of\ molecules\ and\ particles$
$S = Surface\ Reflectance$
$\rho_s = Transmittance\ from\ top\ to\ ground$
$T(\tau_a, \mu_s) = Transmittance\ from\ ground\ to\ TOA$
$T(\tau_a, \mu_v) = Total\ downward\ radiance$
$\mu_s = Cosine\ of\ solar\ zenith\ angle$
$\mu_v = Cosine\ of\ view\ zenith\ angle$
$\emptyset = Cosine\ of\ relative\ azimuth\ angle$
The code was run for specific wavelength ranges, sensor channels, aerosol, and atmospheric models. The input parameters of the LUT are given in Table .1.
In this study the simulated surface reflectance was compared with observed surface reflectance to retrieve the AOD value by lookup table matching. (Jin et al. 2021). AOD was retrieved at a spatial resolution of 500 meters, representing a higher resolution in comparison to existing satellite-derived AOD products.

IV. RESULTS AND DISCUSSION

Due to the unavailability of cloud-free images for all months between the years 2015 to 2023, Seasonal analysis was made to observe the trends in the AOD for February and April months which are shown in Figure. 3a and Fig. 3.b respectively.
From Figure. 3a, it is observed that the AOD levels for each month decreased gradually from 2015 to 2017 with a sudden increase in the year 2018 (Swagata Payra et al. 2021) and a notable decrease during the periods 2020 to 2022. Again in 2023 a gradual increase in the AOD concentration is observed.
From Figure. 3b it is observed that the AOD levels for each month increased gradually from 2015 to 2019 with a notable decrease during the periods 2020 to 2022.
In 2023 again a gradual increase in the AOD concentration is observed.

TABLE I. LOOKUP TABLE INPUT PARAMETERS

Parameter	Units	Range
SOLAR ZENITH	degrees	0, 10, 20, 30, 40, 50, 60, 65, 70, 75
H_2O	g/m2	0, 0.25, 0.5, 1, 1.5, 2, 3, 5, 8.5
O_3	cm-atm	0.0, 0.8
AOD	unitless	0, 0.25, 0.5, 0.75, 1.0, 1.25, 1.5, 2.25, 3
ALTS	Km	0,1,4,7.75
SENSOR CHANNEL	-	LANDSAT OLI
WAVELENGTH	µm	BLUE BAND, RED BAND
AEROSOL MODEL	-	CONTINENTAL MODEL
VIEW ZENITH	degrees	0

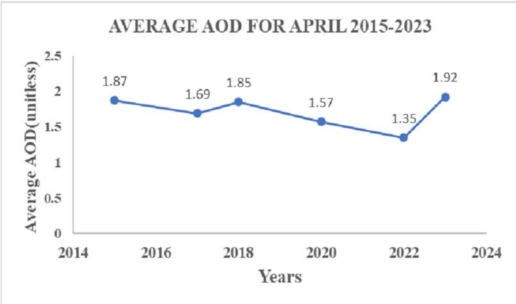

Figure 3. (a) Average AOD for April 2015-2023

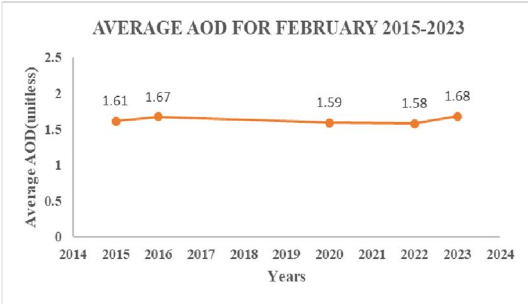

Figure 3. (b) Average AOD for February 2015-2023

Average AOD was computed for April and February months and the peak value was observed in 2023 (1.92) and the least in 2022 (1.35) for April. Due to the non-availability of cloud-free images for February 2017-2019, the trend could not be observed clearly. However, it aligns with the fact that the peak was observed in 2023 (1.68) and the lowest value in 2022 (1.58). According to the Central Pollution Control Board data (CPCB), Chennai had an increase in pollution levels from 2015-2018, and the imposition of the COVID lockdown is believed to be the main reason for the reduction in the Average AOD values from 2020-2022 which was also stated in the study by (Singh 2021). CPCB data of Chennai show a fall in $PM_{2.5}$ levels from 40.86µg/m^3 in 2017 to 28.90µg/m^3 in 2022. Besides the shutdown of industries, reduced traffic conditions were another reason for the decrease in pollution levels according to Times of India dated 27 May 2021. In general, by comparison, it is also observed that the average AOD content in April month has increased compared to February. This can be attributed to the increased high-speed dust particles during summer.

A. Aerosol Optical Depth in Summer

The trend analysis revealed a notable decline in AOD percentage during the year 2020, succeeded by an upturn in AOD values in 2023. The reduction in AOD during 2020 can be attributed to the implementation of lockdown measures, which led to a substantial decrease in air pollution. The commencement of the lockdown in Chennai on March 31, 2020, allowed industries to operate with restricted functionalities, resulting in the cessation of non-essential construction activities while essential projects continued.

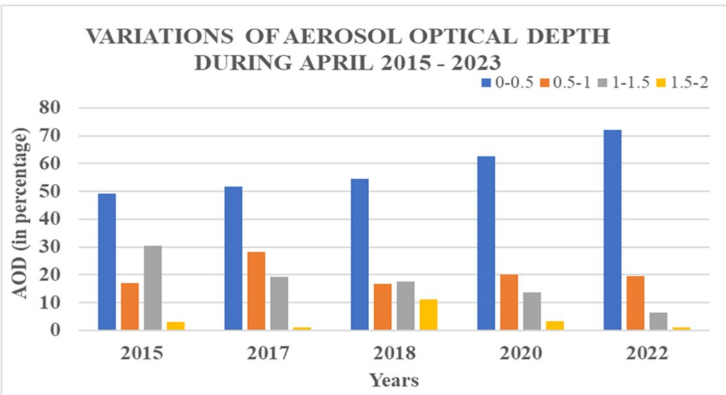

Figure 4. The trend in Aerosol Optical Depth of the April month for the years 2015 – 2023

From Fig 4., it can be observed that there has been a steady increase in the AOD range for the class 0-0.5 from 49% (April 2015) to 62% (April 2020) with a sudden increase in April 2022 (72%). Similarly, there has also been a decrease in the level of AOD for the class 1.5-2.0 from 11% in April 2018, 4% in April 2020 to 2% in April 2022. From Fig.5, it could be observed that pollution concentration was higher in the areas of North Chennai and parts of Perungudi. This may be because of a greater number of thermal power plants in the Northern part of Chennai and landfill areas in Perungudi. The subsequent increase in AOD values in 2023 could be indicative of a return to pre-lockdown levels of human activity or changes in environmental conditions. Additional factors that may contribute to the fluctuations in AOD could be industrial output, shifts in transportation patterns, and alterations in meteorological conditions. A clear decline in AOD can be seen as the year passes due to the increase in the greener areas compared to the red ones.

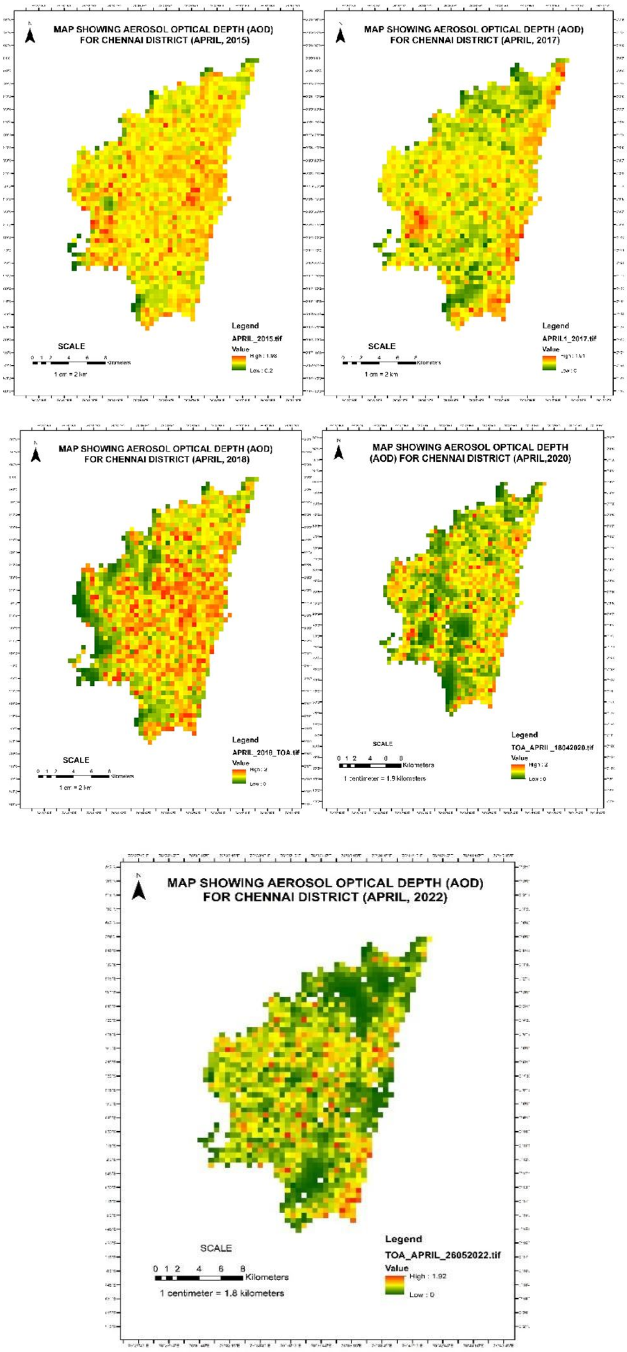

Figure 5. AOD of April month for the years 2015 to 2023

B. Aerosol Optical Depth in Winter

The trend analysis shown in Fig. 6 revealed consistent AOD levels within the range of 0-0.5 over the observed period. In February 2020, there were no significant variations, aligning with the time frame preceding the implementation of lockdown measures. Due to the non-availability of cloud-free images, consecutive year-wise analysis could not be done for February. However, in the subsequent years, there was an observable shift in AOD patterns. Specifically, there was an increase in AOD levels within the range of 0-0.5, accompanied by a concurrent decrease in the 0.5-1 range.

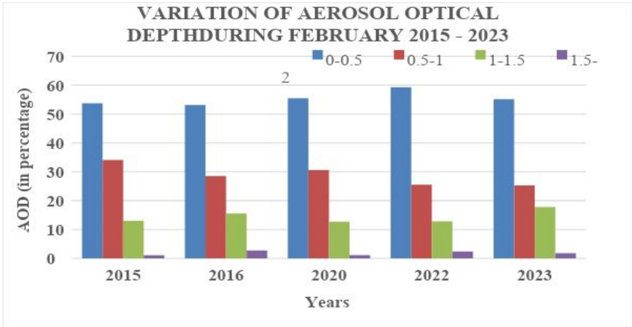

Figure 6. The trend in Aerosol Optical Depth of the February month for the years from 2015 to 2023

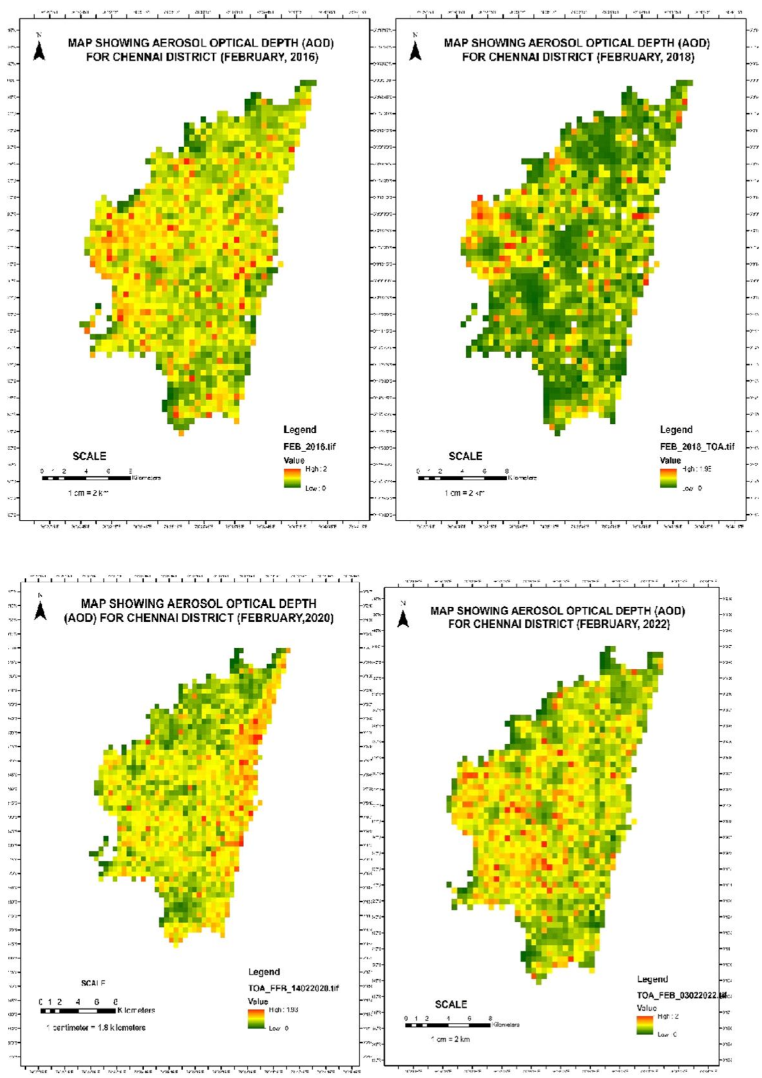

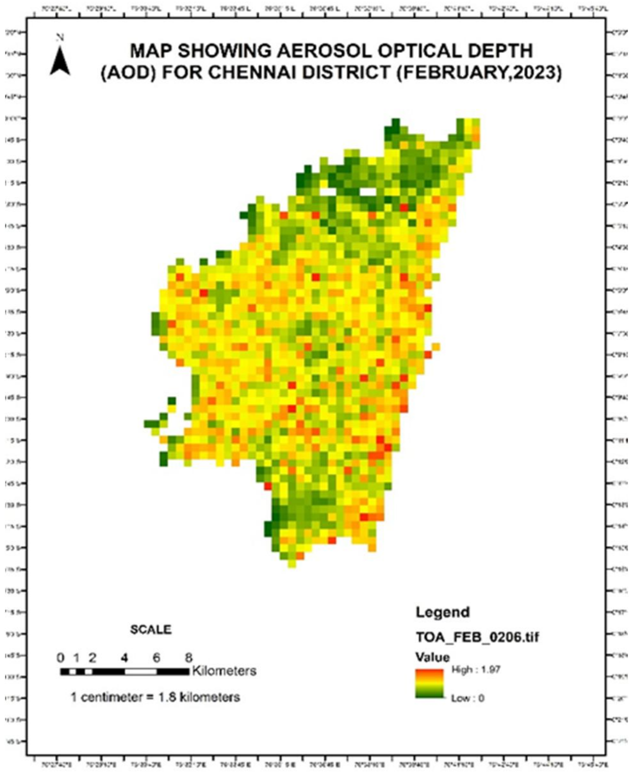

Figure 7. AOD of February for the years 2015 to 2023

Although the change was not much steeper (Figure 7), it could be observed that there has been an increase in the AOD levels of 0-0.5 from 55% (February 2015) observing almost a steady state till 2020 (53% in February 2016 and 56% in February 2020), took a hike in the year 2022 where the percentage of observed AOD was 59%. The reduction in the AOD levels of 0-0.5 in 2023 can be attributed to the fact that the pollution level has increased in the same year (55%). The AOD levels of 1.5-2 almost remained in a steady state ranging from 0.1% in February 2015, 0.4% in February 2016, 0.2% in February 2020, 0.3% in February 2022, and 0.2% in February 2023. Due to the seasonal changes, it can be observed that the AOD levels were comparatively lesser in the winter season than in the summer. As the humidity increases, the size of the particles in the winter season decreases leading to a decrease in the AOD levels. This alteration suggests a noteworthy change in atmospheric conditions and human activities impacting aerosol concentrations during the analyzed period.

C. Validation using $PM_{2.5}$

The validation of AOD has been conducted by comparing with $PM_{2.5}$ data obtained from six ground stations positioned across Chennai is presented in Table 2. In line with prior research that has established a positive association between AOD and $PM_{2.5}$ concentrations (Unnithan et al. 2020), the sensor stations were strategically placed on the AOD map to ensure comprehensive validation, aligning with their corresponding locations. The AOD values obtained were then cross-referenced with the concurrently recorded $PM_{2.5}$ data from the CPCB (Lin et al. 2021). 91 data points were chosen for validating the retrieved AOD. The validation process resulted in an R^2 value of 0.7035 (Figure 8), indicating a significant correlation between AOD and $PM_{2.5}$ values.

TABLE II. VALIDATION SITES

Validation Sites	**Latitude**	**Longitude**
Anna Nagar	13◦09'41.70"	80◦20'39.90"
Thiyagaraya Nagar	13◦04'33.93"	80◦24'21.73"
Adyar	13◦01'24.10"	80◦24'43.52"
Kilpauk	13◦08'02.29"	80◦23'48.52"
Nungambakkam	13◦05'49.29"	80◦23'32.22"

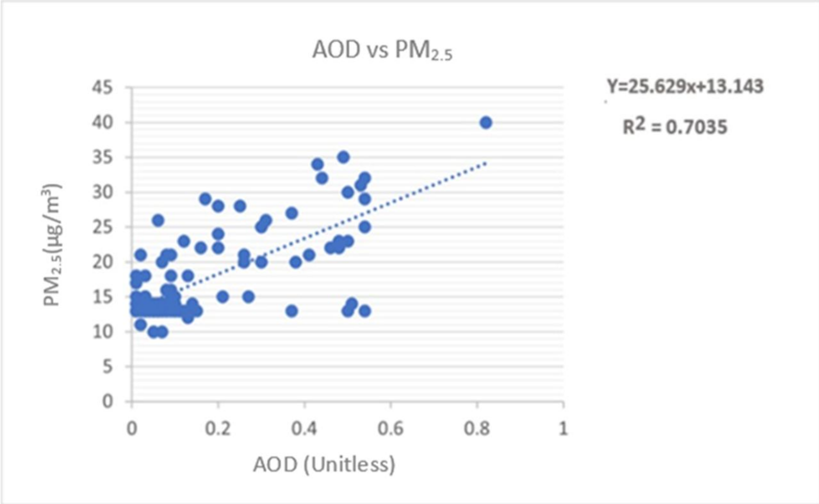

Figure 8. Comparison of AOD and $PM_{2.5}$

V. Conclusion

AOD retrieval using Landsat satellite imagery proves to be a valuable and intricate process. Leveraging Landsat's multi-spectral capabilities, particularly in the blue band, facilitates the estimation of Aerosol Optical Depth in both bright and dark surface areas. The utilization of radiative transfer models, such as the Second Simulation of the Satellite Signal in the Solar Spectrum (6S), combined with the creation of Look-Up Tables (LUTs), enhances the accuracy of surface reflectance determination. The accuracy of Aerosol Optical Depth (AOD) retrieval was found to be more precise in the blue band for bright pixels, while the red band exhibited good accuracy for dark pixels such as vegetation. Combining these two bands through fusion techniques was identified as a strategy to enhance retrieval accuracy across both land and vegetation.

Analysis of AOD maps indicated a decrease in AOD values during the lockdown period, suggesting a reduction in air pollution. Conversely, over corresponding years, air quality demonstrated a decline, with increased AOD values attributed to heightened urbanization. This observation implies a direct correlation between urban development and deteriorating air quality, emphasizing the importance of monitoring atmospheric aerosols for environmental assessment. However, challenges persist, especially in urban landscapes, where factors like complex land cover can complicate AOD retrieval. Careful consideration of solar parameters, and selection of appropriate aerosol and atmospheric models are essential for refining the accuracy of AOD estimates. Also, seasonal-wise variations were observed where the summer season (April – June) had the highest concentration of AOD whereas the winter season had the lowest concentration of AOD.

References

[1] Alexei Lyapustin, Yu Wang, Istvan Laszlo, René S Kahn, Sergey Korkin, Lorraine A Remer, Ronald Levy, and Jeffrey S Reid. 2011. “Multiangle Implementation of Atmospheric Correction (MAIAC): 2. Aerosol Algorithm.” Journal of Geophysical Research 116 (D3). https://doi.org/10.1029/2010jd014986.

[2] Bilal, Muhammad, Janet Elizabeth Nichol, Max Bleiweiss, and David Dubois. 2013. “A Simplified High-Resolution MODIS Aerosol Retrieval Algorithm (SARA) for Use over Mixed Surfaces.” *Remote Sensing of Environment* 136 (September): 135–45. https://doi.org/10.1016/j.rse.2013.04.014.

[3] Chen, Xiangyue, Jianli Ding, Jingzhe Wang, Xiangyu Ge, Mayira Raxidin, Jing Liang, Xiaoxiao Chen, Zipeng Zhang, Xiaoyi Cao, and Yue Ding. 2020. “Retrieval of Fine-Resolution Aerosol Optical Depth (AOD) in Semiarid Urban Areas Using Landsat Data: A Case Study in Urumqi, NW China.” *Remote Sensing* 12 (3): 467. https://doi.org/10.3390/rs12030467.

[4] Jin, Yang-Yang, Zengzhou Hao, Jian Chen, Dong He, Qingjiu Tian, Zhihua Mao, and Delu Pan. 2021. “Retrieval of Urban Aerosol Optical Depth from Landsat 8 OLI in Nanjing, China.” *Remote Sensing* 13 (3): 415–15. https://doi.org/10.3390/rs13030415.

[5] Li, Lili, Jingxue Yang, and Yunpeng Wang. 2014. “An Improved Dark Object Method to Retrieve 500m-Resolution AOT (Aerosol Optical Thickness) Image from MODIS Data: A Case Study in the Pearl River Delta Area, China.” *ISPRS Journal of Photogrammetry and Remote Sensing* 89 (March): 1–12. https://doi.org/10.1016/j.isprsjprs.2013.12.008.

[6] Lin, Hao, Siwei Li, Jia Xing, Tao He, Jie Yang, and Qingxin Wang. 2021. “High-Resolution Aerosol Optical Depth Retrieval over Urban Areas from Landsat-8 OLI Images.” *Atmospheric Environment* 261 (September): 118591. https://doi.org/10.1016/j.atmosenv.2021.118591.

[7] Omari, Khalid, Abdelgadir Abuelgasim, and Khawla Alhebsi. 2019. “Aerosol Optical Depth Retrieval over the City of Abu Dhabi, United Arab Emirates (UAE) Using Landsat-8 OLI Images.” *Atmospheric Pollution Research*, January. https://doi.org/10.1016/j.apr.2019.01.015.

[8] Swagata Payra, Priyanshu Gupta, Rajeev Bhatla, Laaziz El Amraoui, and Sunita Verma. 2021. “Temporal and Spatial Variability in Aerosol Optical Depth (550 Nm) over Four Major Cities of India Using Data from MODIS Onboard the Terra and Aqua Satellites.” *Arabian Journal of Geosciences* 14 (13). https://doi.org/10.1007/s12517-021-07455-y.

[9] Singh, Jyotsna, and Bhishma Tyagi. 2021. “Transformation of Air Quality over a Coastal Tropical Station Chennai during COVID-19 Lockdown in India.” *Aerosol and Air Quality Research* 21. https://doi.org/10.4209/aaqr.200490.

[10] Sun, Lin, Jing Wei, Muhammad Bilal, Xinpeng Tian, Chen Jia, Yamin Guo, and Xueting Mi. 2015. “Aerosol Optical Depth Retrieval over Bright Areas Using Landsat 8 OLI Images.” *Remote Sensing* 8 (1): 23. https://doi.org/10.3390/rs8010023.

[11] Tanre, D., M. Herman, P. Y. Deschamps, and A. de Leffe. 1979. “Atmospheric Modeling for Space Measurements of Ground Reflectances, Including Bidirectional Properties.” *Applied Optics* 18 (21): 3587. https://doi.org/10.1364/ao.18.003587.

[12] Tian, Xin-peng, and Lin Sun. 2016. “Retrieval of Aerosol Optical Depth over Arid Areas from MODIS Data.” *Atmosphere* 7 (10): 134. https://doi.org/10.3390/atmos7100134.

[13] Unnithan, S. L. Kesav, and L. Gnanappazham. 2020. “Spatiotemporal Mixed Effects Modeling for the Estimation of $PM_{2.5}$ from MODIS AOD over the Indian Subcontinent.” *GIScience & Remote Sensing* 57 (2): 159–73. https://doi.org/10.1080/15481603.2020.1712101.

[14] Vermote, E.F., D. Tanre, J.L. Deuze, M. Herman, and J.-J. Morcette. 1997. “Second Simulation of the Satellite Signal in the Solar Spectrum, 6S: An Overview.” *IEEE Transactions on Geoscience and Remote Sensing* 35 (3): 675–86. https://doi.org/10.1109/36.581987.

[15] Wei, Jing, Bo Huang, Lin Sun, Zhaoyang Zhang, Lunche Wang, and Muhammad Bilal. 2017. “A Simple and Universal Aerosol Retrieval Algorithm for Landsat Series Images over Complex Surfaces.” *Journal of Geophysical Research: Atmospheres* 122 (24): 13, 338–313, 355. https://doi.org/10.1002/2017jd026922.

[16] Wei, Jing, Lin Sun, Yiran Peng, Lunche Wang, Zhaoyang Zhang, Muhammad Bilal, and Yanci Ma. 2018. “An Improved High-Spatial-Resolution Aerosol Retrieval Algorithm for MODIS Images over Land.” *Journal of Geophysical Research: Atmospheres* 123 (21): 12, 291–212, 307. https://doi.org/10.1029/2017jd027795.

[17] Wilson, R.T. 2013. “Py6S: A Python Interface to the 6S Radiative Transfer Model.” *Computers & Geosciences* 51 (February): 166–71. https://doi.org/10.1016/j.cageo.2012.08.002.